Limnol. Oceanogr., 44(1), 1999, 80–94
© 1999, by the American Society of Limnology and Oceanography, Inc.

Modeling the relative contributions of autotrophs and heterotrophs to carbon flow at a Lagrangian JGOFS station in the Northeast Atlantic: The importance of DOC

Michael J. R. Fasham[1]
Southampton Oceanography Centre, Waterfront Campus, Southampton SO14 3ZH, U.K.

Philip W. Boyd
NIWA Centre for Chemical and Physical Oceanography, Department of Chemistry, University of Otago, Dunedin, New Zealand

Graham Savidge
Queen's University of Belfast, Marine Laboratory, Portaferry, Northern Ireland BT22 1PF, U.K.

Abstract

A size-structured ecosystem model was developed and fitted to an extensive set of observations of size-fractionated biomass, primary and heterotrophic bacterial production, respiration, particle flux, and zooplankton herbivory obtained on a cruise in the NE Atlantic during 20 days of the spring bloom. Rates of water-column-integrated primary production and heterotrophic bacterial production were used to force the model, and the model parameters were determined by optimizing the model to the remaining observations. A unique model solution was not possible in the absence of dissolved organic carbon (DOC) measurements. By setting a weak constraint on the DOC concentrations (that they should remain broadly constant), a solution was obtained that predicted a small DOC increase during the bloom period; this increase was similar in magnitude to observations in other areas and produced a good fit with the other data. Major conclusions: (1) gross primary production (GPP) was over twice the measured ^{14}C production estimates; (2) phytoplankton exudation was a major source of DOC, and 35% of the GPP flowed through the DOC and was utilized by the bacteria, with a low gross growth efficiency (17%); (3) 62% of the community respiration came from organisms <5 μm in size; (4) the major source of food for microzooplankton was phytoplankton 1–5 μm in size, but the mesozooplankton ingested more microzooplankton than phytoplankton; and (5) only 8% of the total net primary production was grazed by mesozooplankton. These results provide quantitative support to the emerging consensus on the relative roles of large and small organisms in the euphotic zone and demonstrate the necessity of measuring DOC to constrain the carbon budget within the euphotic zone.

A prominent objective of biological oceanography is to determine and understand the processes controlling the fluxes of carbon in the ocean over time. The most important of these is the fate of CO_2 taken up by phytoplankton in the euphotic zone. We wish to quantify how this carbon passes through the food web to its eventual fate as carbon respired within the euphotic zone or carbon exported to the deeper ocean. An attempt to budget carbon was one of the aims of the Joint Global Ocean Flux Study (JGOFS) North Atlantic Bloom Experiment (NABE) carried out in 1989 at a number of stations along the 20°W meridian. The most extensive coverage was at 47°N, where Bender et al. (1992) calculated a carbon budget for the upper water column (0–50 m) over a 13-d period during the spring bloom. Of the total gross primary production of 1.83 mmol C m^{-2}, they estimated that 63% was respired, 16% was stored as particulate organic carbon (POC) within the upper 50 m, and 18% was sedimented out to depths >50 m.

Bender et al. (1992) did not attempt to unravel the details of how the carbon flowed through the euphotic zone food web, which would require more quantitative information on how primary production is partitioned among size classes, the fraction of primary production grazed by small and large zooplankton, and the role of dissolved organic carbon (DOC) and heterotrophic bacteria. In this study, we evaluated carbon flow using data from a U.K. JGOFS 1990 cruise centered on 47°N, 18°W in the northeast Atlantic. This cruise was carried out in Lagrangian mode by following a drifting buoy in an attempt to minimize the effects of horizontal advection; several biomasses and fluxes were measured over a 20-d period. However, the measurement set was not sufficiently complete to allow carbon budgets to be constructed on a daily basis, so a new size-structured ecosystem model was developed; the components of this model matched the observation set and were fitted to these observations using a nonlinear parameter estimation technique (Fasham and Evans 1995, 1998). This ecosystem model draws on previous size-structured models (Ducklow and Fasham 1991; Taylor et al. 1993) but differs in that it uses the daily observations of bacterial production and size-fractionated primary production as forcing functions and models the subsequent fate of these inputs as they pass up the food web. The model results were then used to produce self-consistent carbon budgets and quantify the various pathways for carbon flow within the euphotic zone.

[1] Corresponding author: mjf@soc.soton.ac.uk.

Acknowledgments

We thank those colleagues in the UK BOFS Program who provided data for this study and also the staff of the British Oceanographic Data Centre for assistance with accessing the BOFS database. This article is BOFS Contribution 275.

Table 1. The quantities measured, techniques used and frequency of sampling during the 1990 BOFS Lagrangian study. Sources refers to the published work containing comprehensive details of the methods used during this study.

Parameter	Technique	Frequency	Source
Size-fractionated chlorophyll *a*	Fluorescence	Daily	Savidge et al. (1995)
Size-fractionated primary production	^{14}C	Daily	Savidge et al. (1995)
Heterotrophic bacterial biomass	DAPI	Daily*	Kirchman et al. (1993)
Heterotrophic bacterial production	^{3}H-TdR	Daily*	Kirchman et al. (1993)
Microzooplankton biomass	DAPI, proflavin	Irregular	Burkill et al. (1993)
Microzooplankton grazing	Dilution method	Alternate days	Burkill et al. (1993)
Mesozooplankton biomass	Net hauls	Alternate days	Morales et al. (1993)
Mesozooplankton grazing	Gut fluorescence	Alternate days	Morales et al. (1993)
Community respiration	Micro-Winkler O_2	Alternate days	Williams (1981*b*)
Vertical carbon flux	^{234}Thorium	1 per 4 days	Ritchie and Shimmield (1991)
Nitrate concentration	Autoanalyzer	2–6 per day	

* Observations in which sampling was occasionally less frequent than stated.

Methods

The data—The data were obtained from the first of a two cruise Lagrangian experiments centered on 47°N, 18°W as a component of the Biogeochemical Ocean Flux Study (BOFS), a U.K. contribution to JGOFS. The site was occupied from 1 May (day 121) to 20 May 1990 (day 140), during which time the ship tracked a drogued buoy that had been placed in an anticyclonic eddy identified from a large scale SeaSoar survey (Savidge et al. 1992). During this period, serial sampling of the water column was carried out, and a set of biogeochemical variables was measured using the methods presented in Table 1. The frequency of sampling ranged from daily to weekly for different variables.

Size-fractionated chlorophyll *a* concentration and primary production, heterotrophic bacterial biomass, heterotrophic bacterial production, and community respiration were determined from common water samples taken before dawn at six depths in the upper 35 m of the water column (corresponding approximately to the depth of the mixed layer). Phytoplankton primary production was estimated from 24-h ^{14}C incubations and are assumed to be a measure of net primary production (Laws 1991; Chipman et al. 1993). In the absence of any direct measurements, a carbon : chlorophyll *a* ratio of 50 was assumed and used to convert phytoplankton chlorophyll *a* concentrations to units of carbon (Gieskes 1991). Bacterial biomass and production were converted to carbon using a conversion constant of 20 fgC cell^{-1} and 2×10^{18} cells produced per mole of thymidine incorporated (Kirchman et al. 1993).

The size fractions for phytoplankton biomass and production were 0.2–1 μm, 1–5 μm, and >5 μm, designated picophytoplankton, nanophytoplankton, and microphytoplankton, respectively, although these size fractions do not exactly correspond to the standard definition of these terms (Sieburth et al. 1978). The size classes were chosen to reflect the food web structure of the NE Atlantic, especially the fact that copepods cannot graze efficiently on cells ≤ 5 μm in size (Joint and Williams 1985; Berggeren et al. 1988).

The data are presented as daily integrated values (0–35 m). To standardize the data sets to this format it was necessary to make some assumptions. For heterotrophic bacterial production, which was based on 4-h incubations, the values have been extrapolated to obtain 24-h production estimates. Microzooplankton and mesozooplankton biomass estimates are based on vertical net hauls from 0–35 m and from 0–100 m, respectively. The grazing rates derived for microzooplankton and mesozooplankton were obtained from either 10-m or 25-m samples. For microzooplankton herbivory the rates from one depth were assumed to be representative of the mixed layer population and were scaled accordingly to obtain a column integrated value. The mesozooplankton biomass was measured over the upper 100 m of the water column. However, because they exhibit diel vertical migration (Morales et al. 1991), mesozooplankton from 0–100 m probably would graze predominantly in the surface mixed layer (0–35 m); therefore, the mesozooplankton grazing rates have been scaled to the 0–100-m population but applied to the 0–35-m water column.

The estimates of the downward flux of POC are based on ^{234}Th disequilibria. Thorium data were collected from 0–50 m and thus represent the flux of material exiting a 50-m water column; the magnitude of this flux has been assumed to be not significantly different from that leaving the surface mixed layer (0–35 m).

Samples for DOC analysis were obtained on the cruise, but because of problems with the high temperature oxidation technique at sea, these data were unusable. This problem with the DOC analysis severely limited our ability to produce a uniquely determined carbon budget.

Development of the bloom—During the first 10 d of the Lagrangian experiment, the chlorophyll *a* concentrations ranged between 0.6 and 2.1 mg m^{-3} in the mixed layer, with no obvious temporal trend, whereas nitrate concentrations decreased from 6.1 to 3.6 mmol m^{-3} (Fig. 1A). There was a progressive development of the stratification of the seasonal thermocline between depths of 20 and 35 m over the 20-d period, with surface temperatures increasing from 12°C to 14°C (Savidge et al. 1992, fig. 9). Starting around 8 May (day 128), the phytoplankton production in all three size fractions began to show an upward trend (Fig. 1B), although there were large day-to-day variations. Apart from the observations at the beginning of the cruise and on 15 May (day 135), the variability in production was correlated with daily averaged photosynthetically available radiation (PAR) esti-

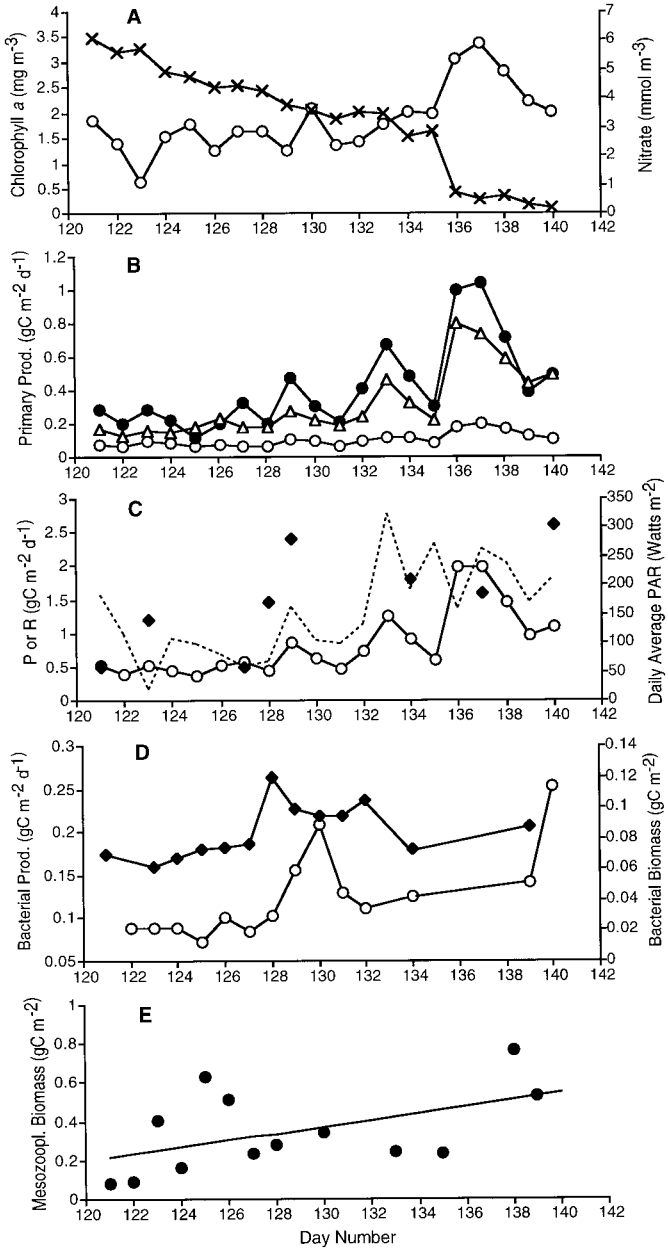

Fig. 1. Temporal change of key observations within the mixed layer (0–35 m) during the Lagrangian experiment. (A) Total chlorophyll *a* (circles, mg m^{-3}) and nitrate concentrations (crosses, mmol N m^{-3}). (B) ^{14}C primary production estimates (gC m^{-2}) in the size fractions <1 μm (○), 1–5 μm (●), and >5 μm (△). (C) Total primary production in all three size classes (gC m^{-2}, ○) and community respiration (gC m^{-2}, ♦). The daily average PAR (Watts m^{-2}) is shown by a dashed line. (D) Bacterial production (gC m^{-2} d^{-1}, ○) and bacterial biomass (gC m^{-2}, ♦). (E) Mesozooplankton biomass (gC m^{-2}). The regression line of biomass against day number is also shown.

mates (Fig. 1C), and over the whole 20 d the variance in PAR accounted for 50% of the variance in production (significant at the 1% level). The eight observations of community respiration showed little correlation with the ^{14}C estimates of primary production (Fig. 1C), although there was a significant (5% level) increase over the whole 20 d. The ratio of daily community respiration to ^{14}C production ranged between 0.8 and 3.2 (mean ± SE = 1.9 ± 0.9).

On 16 May (day 136), the phytoplankton biomass increased sharply, accompanied by a decline in mixed layer nitrate (Fig. 1A). In the last 3d of the experiment, both the phytoplankton biomass and the rate of nitrate utilization declined.

Both bacterial production and biomass increased somewhat over the first 10 d, although the increase in biomass occurred before the increase in production (Fig. 1D). In the latter part of the period, the data were too sparse to allow any conclusions to be drawn. Over the whole 10 d, bacterial production averaged 20% of the ^{14}C production.

The mesozooplankton biomass was very variable (Fig. 1E), and although a regression with time gives a positive trend of 19 mgC m^{-2} d^{-1}, it only explained 25% of the variance (significant at 5% level). The observations of microzooplankton biomass were too few to allow any firm conclusions to be drawn (*see* Fig. 4b).

The problem of advection—One of the aims of this study was to budget the carbon flow over the period of the Lagrangian experiment. If the effects of physical mixing or advection are neglected, then over the whole 20 d the gross primary production (GPP) must be balanced by the sum of the community respiration, any increase in organic carbon (DOC + POC) within the top 35 m, and any export from the 0–35-m layer, i.e., the downward POC flux. The survey plan was designed to minimize the effects of advection by following a drifting buoy. In any realistic flow field, it is impossible to completely remove advective fluxes by such a simple expedient, but we need to establish that such fluxes are indeed small compared with the other ecosystem fluxes that affect the carbon budget.

In the first analysis of these data, Savidge et al. (1992) thought that advection could be significant. They compared the changes in nitrate concentration in the top 35 m with that predicted from ^{15}N uptake experiments during 8–16 May and concluded that the day-to-day correlation between the two measurements was poor; on three occasions there was an increase in nitrate concentration as compared with the previous day. Thus, they conclude that advection did play a significant role in the temporal changes of nitrate and, by implication, other biological variables. Two problems with this analysis need to be addressed before these conclusions about advection can be accepted. First, the nitrate uptake data were calculated by extrapolating from surface values only; however, the complete data set is now available (Boyd et al. 1995), with NO_3 uptake measurement from six depths in the top 35 m on 8 days (1, 3, 7, 9, 11, 14, 17, and 19 May). The second problem is that the daily changes in nitrate were based on just two hydrocasts taken concurrently with sampling for the ^{15}N experiment. The estimation of the average nitrate concentration in the top 35 m using such hydrocasts will be subject to measurement errors and can also be greatly affected by variations in the depth of the nitricline due to internal waves (Holligan et al. 1985). One way of ameliorating this problem is to use all the hydrocasts for a given day to calculate a daily average. Even when this ap-

proach was taken, the nitrate concentration still showed an increase on three of the days (Fig. 1A). However, the total calculated decrease in nitrate between 1 and 20 May was 113 ± 42 mmol N m^{-2}. Summing the nitrate uptake calculated from the ^{15}N experiments for the same period, using the full NO_3 uptake data set, gives 92 mmol N m^{-2}, not significantly different from the decrease in nitrate concentration. Although this agreement does not prove conclusively that advection is unimportant, it does suggest that advective effects were small compared with the larger biological fluxes during the bloom.

The ecosystem model

Model equations—The data set described can be used to define a model ecosystem with seven state variables: picophytoplankton, nanophytoplankton, microphytoplankton, microzooplankton, mesozooplankton, and heterotrophic bacteria; for all of these components there are observations at various frequencies. In addition, a state variable for DOC is included, although there are no observations of this quantity. Any detritus that is produced (i.e., mesozooplankton fecal pellets) is assumed to sink immediately from the surface 35 m and form part of the downward POC flux. In reality, some detritus may not sink rapidly and will accumulate within the mixed layer and contribute to the increase in POC; therefore, strictly speaking, an extra model component for such detritus should be included. However, because we have no measurements of detrital concentrations and because any mixed layer detritus will be recycled to dissolved inorganic carbon or DOC over a fairly short time, it seems more reasonable to subsume this slow sinking detritus within the model DOC pool.

In addition to measurements of state variable concentrations, there are measurements of eight fluxes; net primary production (NPP) for all three phytoplankton size classes, bacterial production, autotrophic grazing by micro- and mesozooplankton, total community respiration, and downward POC flux out of the mixed layer. The flow diagram for the model is shown in Fig. 2.

We attempted to simulate effectively the observed data set and then to use the model results to determine the full set of carbon flows within the mixed layer ecosystem over the 20-d experimental period. We particularly examined the extent to which inputs to the system are balanced by outputs and the role of the various compartments in the mixed-layer carbon flows. One of the classic ways to analyze material flows in a system is input–output flow analysis (Ducklow et al. 1989). In this technique, the output flow of carbon from a compartment is partitioned into respiration, DOC production, detritus, and predation to higher trophic levels; these flows are then assumed to be constant fractions of the input flow. Using simple matrix arithmetic, it is then possible to calculate a complete flow matrix for any food web given the input flows (Fasham 1985). The advantage of flow analysis is that it requires a relatively small number of parameters to define the system. However, the method assumes a steady state system and so is not strictly applicable to a spring bloom. Another approach would be to use a classical marine ecosystem model in which rate-specific parameters are defined for all compartments, and intercompartment flows are functions of the compartmental concentrations (e.g., Ducklow and Fasham 1991). We used a hybrid approach, using the observed values of phytoplankton and bacterial production as given forcing inputs and then producing a model to analyze the fate of this production. Some flows such as respiration, DOC excretion, and fecal pellet production are assumed to be constant fractions of the input flow to a compartment, whereas others such as predation and phytoplankton sinking are biomass dependent. Obviously, other choices could have been made; for example, respiration could be biomass dependent. The final model was chosen based on its ability to give the best overall fit to the observations. Another simplification of this model was that difference equations instead of differential equations were used because biomass and production were only measured daily at most.

The basis of the model is a submodel of the carbon flows through a generic compartment given an index i. The total input to this ith compartment on day t is defined as T_{it} (the i indices used for the compartments are defined in Table 2; in addition, indices 0 and 8 are assigned to respiration and downward POC flux, respectively). The inputs for the phytoplankton and bacteria compartments are the gross production derived from the observed ^{14}C primary production and thymidine bacterial production values (*see* next paragraph). The input for each zooplankton compartment is the sum total of all the calculated grazing terms.

There are four other assumptions of the model. First, respiration and DOC excretion for all biotic compartments are fractions c_{i0}, c_{i7}, respectively, of the input flow T_{it}. It has been assumed that the observed ^{14}C primary production values are measures of net production, and so the input term for the phytoplankton components will be the $T_{it} = P_{it}/(1 - c_{i0} - c_{i7})$, $i = 1, 3$. The phytoplankton respiration and DOC excretion are then given by $c_{i0}T_{it}$ and $c_{i7}T_{it}$. In the case of bacteria, it was assumed that there is no net DOC excretion, so the input is $T_{6t} = P_{6t}/(1 - c_{60})$ and respiration is $c_{60}T_{6t}$.

Second, microphytoplankton sink with sinking rate V_3 (m d^{-1}). Small phytoplankton and bacteria are assumed not to sink, and zooplankton are assumed to be able to maintain their position within the water column.

Third, fecal pellet production of mesozooplankton is assumed to be a constant fraction of the input flow and to contribute directly to the downward POC flux without any remineralization taking place. However, mesozooplankton mortality is excluded from the downward POC flux. Microzooplankton feces have very low sinking rates and have a high probability of being remineralized in the mixed layer (Stoecker 1984). This characteristic was parameterized in the model by assuming that microzooplankton fecal pellet production could be subsumed within the DOC production term. Thus, the gross growth efficiency (GGE) is $1 - c_{50} - c_{57} - c_{58}$ for mesozooplankton and $1 - c_{40} - c_{47}$ for microzooplankton.

Fourth, predation is parameterized by a multiple resource generalization of the Holling type II function. Total food F available to the predator j is defined as a weighted sum of the prey, thus $F = \Sigma\, c_{kj}\, B_{kt}$, where c_{kj} are grazing preferences

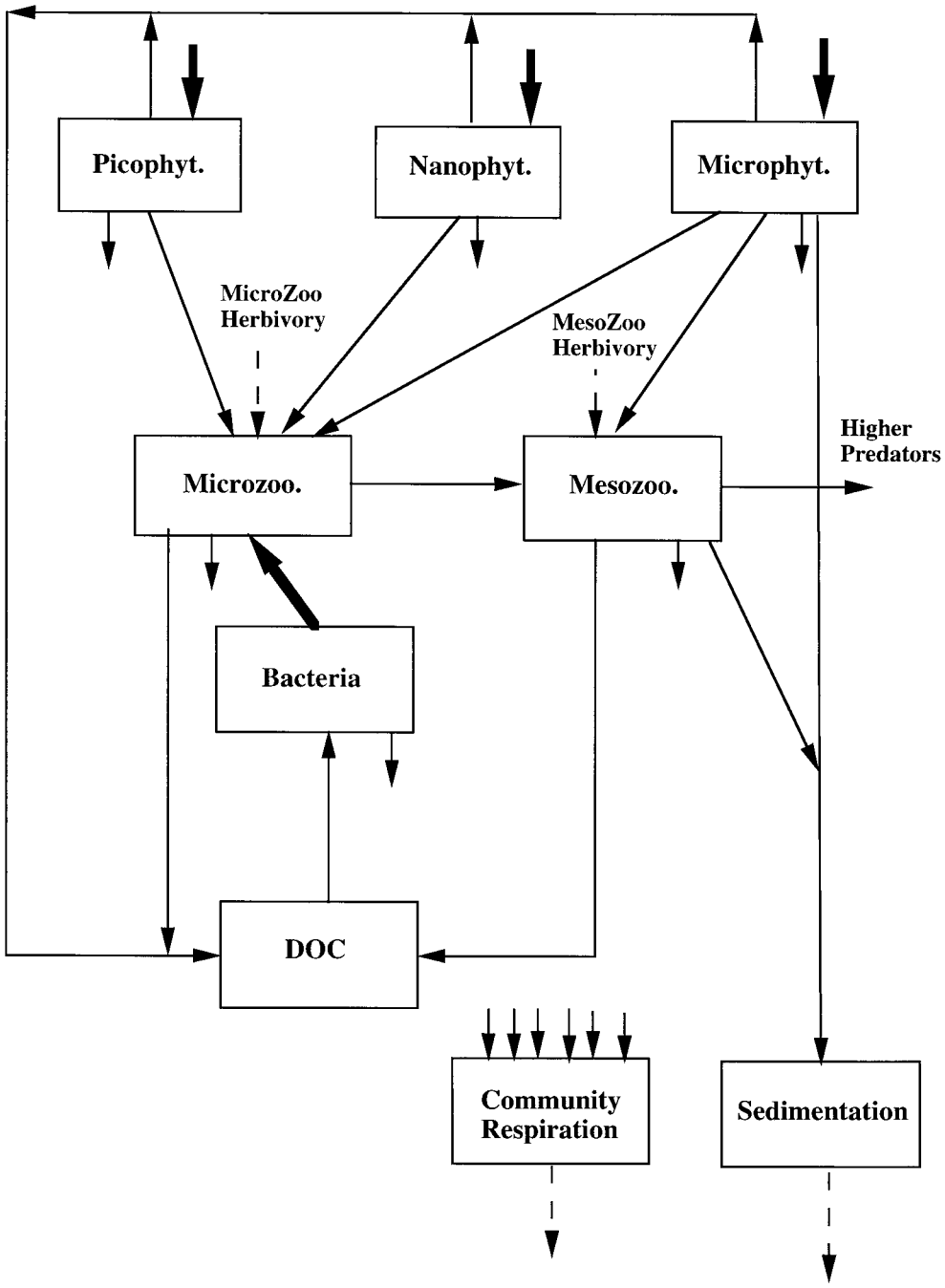

Fig. 2. Diagrammatic flow diagram of the ecosystem model. The thick lines show the observed flows used to force the model, and the dashed lines are the observed flows used, in conjunction with the biomass observations, to optimize the model solution.

(these preferences are the inverse of the half-saturation constants), B_{kt} is the prey concentration (gC m^{-2}) on day t, and the summation is over all prey types. The specific grazing rate (d^{-1}) of predator j on prey i is then given by

$$G_{ij} = \frac{g_j c_{ij} B_{it}}{1 + F}, \tag{1}$$

where g_j is the maximum grazing rate (d^{-1}). Microzooplankton can prey on all three classes of phytoplankton and heterotrophic bacteria, but mesozooplankton are assumed to prey only on phytoplankton >5 μm (Joint and Williams 1985) and microzooplankton.

The equations for pico- and nano-phytoplankton are given by

$$B_{it'} = P_{it} + B_{it} - G_{i4} B_{4t}, \qquad i = 1, 2 \tag{2}$$

where $t' = t + 1$ and P_{it} is the observed NPP (gC m^{-2} d^{-1}) on day t. This equation simply states that the biomass at

Table 2. Index numbers of compartments and output flows.

Index	Compartment
1	Picophytoplankton (<1 μm)
2	Nanophytoplankton (1–5 μm)
3	Microphytoplankton (>5 μm)
4	Microzooplankton (<200 μm)
5	Mesozooplankton (>200 μm)
6	Bacteria
7	DOC
8	Downward POC flux
0	Respiration

time $t + 1$ is the biomass at time t plus the net production less the predation by microzooplankton.

The microphytoplankton are grazed by micro- and mesozooplankton and can also sink. The equation is therefore

$$B_{3t'} = P_{3t} + B_{3t}(1 - V_3/M) - G_{34}B_{4t} - G_{35}B_{5t}, \quad (3)$$

where M is the mixed layer depth, in this case 35 m.

The equation for heterotrophic bacteria is

$$B_{6t'} = P_{6t} + B_{6t} - G_{64}B_{4t}, \quad (4)$$

where P_{6t} is the observed bacterial production on day t.

The microzooplankton equation is

$$B_{4t'} = B_{4t}\left[1 + \left(\sum_{i=1}^{3} G_{i4} + G_{64}\right)(1 - c_{40} - c_{47})\right] - G_{45}B_{5t}. \quad (5)$$

Thus the increase in biomass is given by the input from predation multiplied by the GGE less the predation by mesozooplankton.

The equation for mesozooplankton is

$$B_{5t'} = B_{5t}[1 + (G_{35} + G_{45})(1 - c_{50} - c_{57} - c_{58}) - \mu_5 B_{5t}]. \quad (6)$$

The equation for mesozooplankton differs from that for microzooplankton in that a density-dependent mortality term, $\mu_5 B_{5t}^2$, has been subtracted to provide a closure for the model. It is further assumed that this mortality flux is mainly due to higher predators and so, over the time scale of the observations, it is an export from the system that does not form part of the downward POC flux.

The equation for DOC is

$$B_{7t'} = B_{7t} + \sum_{i=1}^{5} c_{i7}T_{it} - P_{6t}/(1 - c_{60}). \quad (7)$$

Thus, the DOC change is the sum of increases due to DOC release by phytoplankton and zooplankton less the uptake by bacteria.

Equations for community respiration, downward POC flux, and micro- and mesozooplankton herbivory can now be written; these fluxes are required for the optimization against their observed values:

$$\text{community respiration} = \sum_{i=1}^{6} c_{i0}T_{it} \quad (8)$$

$$\text{downward POC flux} = V_3B_{3t}/M + c_{58}T_{5t} \quad (9)$$

$$\text{microzooplankton herbivory} = \sum_{i=1}^{3} G_{i4}B_{4t} \quad (10)$$

$$\text{mesozooplankton herbivory} = G_{35}B_{5t}. \quad (11)$$

The downward POC flux is given by the sum of microphytoplankton direct sinking and zooplankton fecal pellet production.

Fitting the model to the observations—The model parameters were estimated from observations using a nonlinear estimation technique (Fasham and Evans 1995). A penalty function T is defined that measures the misfit between the model and the data, and then this function is minimized by adjusting the parameter values using a nonlinear optimization method. The penalty function used was the sum of a measure of model misfit to the observations T_{obs} and a measure of parameter misfit T_{par}, which is included to ensure that the optimized parameters remain within reasonable bounds:

$$T_{obs} = \sum\sum \frac{w_{ij}(Xobs_{ij} - Xmod_{ij})^2}{Xmod_{ij}^{\ 2}}, \quad (12)$$

where $Xobs_{ij}$ and $Xmod_{ij}$ are the observed and simulated values, respectively, of a state variable i at time t_j and w_{ij} is a weight; the double summation is over all the state variables and all observation times. Unlike the penalty function used by Fasham and Evans (1995), this function is nondimensional because of the difference in units between the biomass and flux observations. Weights of 10 and 1 were given to the biomass observations and the flux observations, respectively. The solution obtained will be affected by the choice of weight values; experiments with different weighting sets showed that the model solutions for variables with good data coverage were little affected, whereas the solutions for data-poor variables, such as microzooplankton, were more variable. The final choice of weights was based on our assessment that the biomass observations (especially the phytoplankton biomass) were more reliable than the flux observations and that it was more important that the model gave a good fit to the former.

Before defining T_{par}, the parameter space is transformed into one more useful for carrying out the optimization process. T is the suggested or target value of the parameter, and U and L are its upper and lower bounds, respectively. If p is any model parameter value, then a variable q is defined as

$$q = \frac{T - p}{L - p} \qquad L \le p < T \quad (13)$$

$$q = \frac{p - T}{U - p} \qquad T \le p \le U. \quad (14)$$

Thus the parameter p that varies over the range (L, U) is transformed into the variable q varying over the range ($-\infty$,

Table 3. Parameter values (mean ± SE) determined for the two models used in the analysis. Also given are the lower (L), upper (U), and target (T) values of the parameters used in the optimization procedure.

Parameter	T	L	U	Model 1	Model 2
c_{14}	1.0	0.0	2.0	0.72 ± 0.10	0.62 ± 0.12
c_{17}	0.05	0.0	0.5	0.33 ± 0.34	0.05 ± 0.41
c_{10}	0.1	0.0	0.3	0.21 ± 0.20	0.09 ± 0.69
c_{24}	1.0	0.0	2.0	0.29 ± 0.04	0.25 ± 0.05
c_{27}	0.05	0.0	0.5	0.36 ± 0.14	0.05 ± 0.36
c_{20}	0.1	0.0	0.3	0.23 ± 0.10	0.07 ± 0.30
c_{34}	1.0	0.0	2.0	0.14 ± 0.03	0.12 ± 0.03
c_{35}	1.0	0.0	2.0	0.51 ± 0.14	0.50 ± 0.15
c_{37}	0.05	0.0	0.5	0.33 ± 0.26	0.05 ± 0.35
V_3	0.1	0.0	2.0	1.50 ± 0.62	1.51 ± 0.57
c_{30}	0.1	0.0	0.3	0.22 ± 0.15	0.08 ± 0.37
c_{45}	1.0	0.0	1.0	1.85 ± 0.11	1.79 ± 0.15
c_{47}	0.1	0.0	0.5	0.21 ± 0.05	0.28 ± 0.07
c_{40}	0.5	0.0	0.8	0.55 ± 0.05	0.51 ± 0.07
g_4	1.0	0.5	3.0	1.64 ± 0.21	2.01 ± 0.36
c_{57}	0.1	0.0	0.3	0.19 ± 0.05	0.08 ± 0.04
c_{58}	0.25	0.2	0.3	0.29 ± 0.03	0.28 ± 0.04
c_{50}	0.45	0.4	0.7	0.45 ± 0.01	0.56 ± 0.07
g_5	0.3	0.1	0.5	0.46 ± 0.02	0.46 ± 0.02
μ_5	0.1	0.0	0.5	0.03 ± 0.03	0.04 ± 0.03
c_{64}	1.0	0.0	2.0	1.74 ± 0.23	1.49 ± 0.29
c_{60}	0.7	0.3	1.0	0.83 ± 0.04	0.90 ± 0.04
B_1	0.3	0.1	0.5	0.26 ± 0.04	0.26 ± 0.04
B_2	1.5	1.0	2.0	1.30 ± 0.13	1.32 ± 0.13
B_3	0.6	0.3	0.7	1.01 ± 0.09	1.01 ± 0.08
B_4	0.6	0.3	0.7	0.53 ± 0.05	0.49 ± 0.10
B_5	0.1	0.05	0.6	0.44 ± 0.03	0.44 ± 0.03
B_6	0.075	0.05	0.1	0.07 ± 0.01	0.07 ± 0.01

$+\infty$); this transformation makes it much easier to use standard optimization subroutines while ensuring that the parameters do not take on ecologically unrealistic values.

The penalty function T_{par} is then defined as $T_{par} = \Sigma\ q^2/v$, where v is an estimate of the parameter variance and the summation is over all the parameters. The variance v is chosen such that T_{par} is similar in magnitude to T_{obs}; a value of 10 was used but the results are not sensitive to even order of magnitude changes in v. The values of T, L, and U are given in Table 3.

To obtain a solution, initial values of the parameter set are first defined (usually the target values), and then the model is run for 20 d and the penalty function $T_{tot} = T_{obs} + T_{par}$ is calculated. Powell's derivative-free conjugate gradient method (Press et al. 1992) was then used to iterate to a minimum T_{tot}.

Once a minimum has been found it is possible to calculate the variance and covariances of the parameters (Gill et al. 1981) by calculating the inverse of the Hessian matrix defined as $|\partial^2 T_{tot}/\partial_{p_i}\ \partial_{p_j}|$. In practice, the Hessian matrix was first calculated in the q space using a centered difference approximation with an iterative process to determine the step size (Gill et al. 1981). The Hessian matrix was then transformed into the parameter space using the chain rule before inverting the matrix. The variance of the parameters is then given by the diagonal of this inverted matrix.

During the initial runs, it soon became apparent that without the constraint of the DOC concentrations it was not possible to obtain a unique solution for the model parameters. It was therefore decided to focus on two solutions using very different assumptions about the DOC concentrations. For one solution (model 2), no constraint of any sort was placed on DOC; and the DOC concentration declined almost linearly over the 20-d period. This result runs counter to most observations of DOC changes during the spring bloom. To investigate the possibility of an alternative solution (in which DOC does not decrease), the DOC concentrations were weakly constrained to be broadly invariant with time (model 1) by adding to the observation set before optimization some extra constant DOC "observations" (with weight = 1) for every odd-numbered day. Thus, the optimization would attempt to find a solution with constant DOC but, because of the low overall weight of these DOC "observations," solutions in which DOC does not remain constant can still be obtained. The total number of parameters optimized for both cases (including the initial values of phytoplankton, zooplankton, and bacteria biomass) was 28.

Results

Model 1: DOC constrained—The optimized parameter values and their standard errors are shown in Table 3. A few of the parameters (c_{17}, c_{10}, μ_5) have standard errors that are of the same magnitude or are larger than the parameter values themselves. Thus, these parameters cannot be accurately estimated from the available data set. In fact, when these parameters were set to zero before the optimization, then the resulting fit to the observations was almost as good as that obtained when these parameters were allowed to vary.

A comparison of the predicted and observed changes in phytoplankton biomass for the three size classes is provided in Fig. 3. The modeled picophytoplankton population shows a decline over the first 10 d that is in good agreement with the observations. This decline is followed by a period of little change, followed by a bloom beginning on day 136 and then a decline over the last 2 d. The model picophytoplankton bloom is due to an increase in production (Fig. 1B), but the predicted increase in biomass is not supported by the observations (Fig. 3a). The modeled nano- and microphytoplankton biomasses show a very small increase over the first 10 d, followed by more rapid growth starting on day 133 that levels off or declines on the last 2 d (Fig. 3b,c). The model reproduces the bloom of both nano- and microphytoplankton quite well, although the modeled peak in the bloom occurs 1–2 d after the observed peak, and the subsequent decline in the observed biomass is not fully matched by the model (especially for microphytoplankton).

Modeled bacterial biomass changed little over time (Fig. 4a) apart from on days 130–131. The predicted bloom over this period was caused by the high bacterial production on days 129–130, (Fig. 1D), but there is no indication of such a bloom in the actual bacterial biomass. By day 132, an increase in microzooplankton grazing in the model restores the biomass values back to the observed levels.

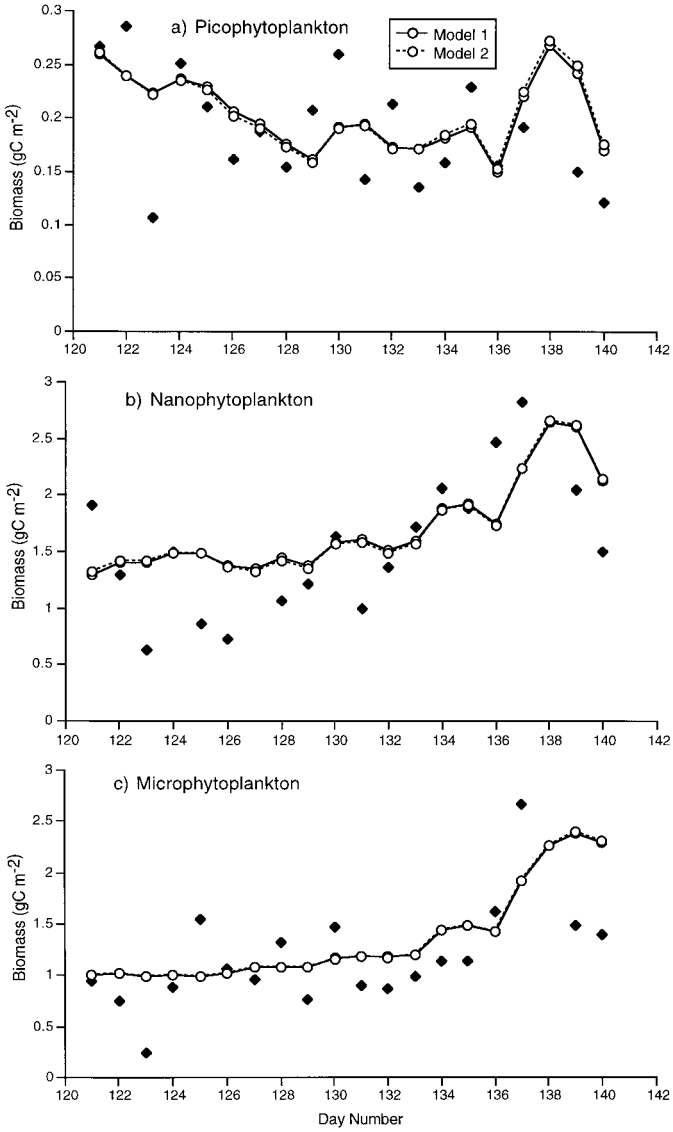

Fig. 3. Modeled phytoplankton biomass (gC m^{-2}) predicted by model 1 (solid lines) and model 2 (dashed lines) compared with observations: (a) picophytoplankton, (b) nanophytoplankton, (c) microphytoplankton. In this and subsequent figures, observations are plotted as diamonds.

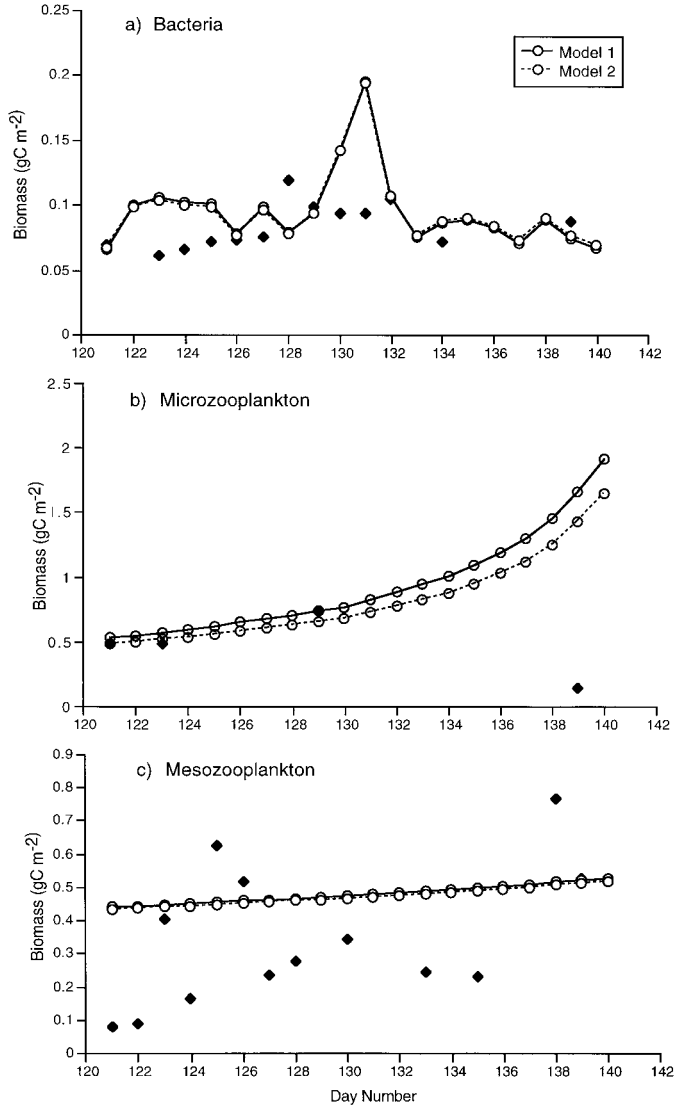

Fig. 4. Modeled biomass of (a) bacteria, (b) microzooplankton, and (c) mesozooplankton compared with observations. All units are gC m^{-2}.

The modeled microzooplankton and mesozooplankton biomasses both increase over the 20 d (Fig. 4b,c). However, the increase in modeled mesozooplankton biomass over the 20 d (0.09 gC m^{-2}) is less than that predicted by a regression of the observed biomass against time (Fig. 1E; 0.33 ± 0.17 g C m^{-2} over 18 days) but it is within the 95% confidence limits. There were only four observations of microzooplankton biomass (Fig. 4a), and so validation is extremely difficult for this variable, although the model almost exactly reproduces the increase in microzooplankton biomass up to day 129. Thereafter, the model microzooplankton biomass increases by a factor of 2.6, but the only observation (day 139) has a value less than any of the previous observations. Because microzooplankton grazing is usually closely coupled with primary production (Burkill et al. 1993), one would expect microzooplankton biomass to increase during the bloom unless these organisms were closely controlled by grazing. This argument might therefore cast some doubt on the reliability of the last microzooplankton biomass measurement. The modeled GGEs for micro- and mesozooplankton and bacteria were 24% ± 5%, 7% ± 6%, and 17% ± 4%, respectively.

Model 1 provides a good fit to the observations of the rates of microzooplankton herbivory for the first 13 d of observations (Fig. 5a). Subsequently, the modeled grazing rates more than double because of the increased prey and microzooplankton biomass concentrations, whereas the observations did not show such an increase. Modeled mesozooplankton herbivory rates increased only slightly over the 20-d period and are within the range of the observations, which show no consistent trend (Fig. 5b).

As might be expected given the increase in overall com-

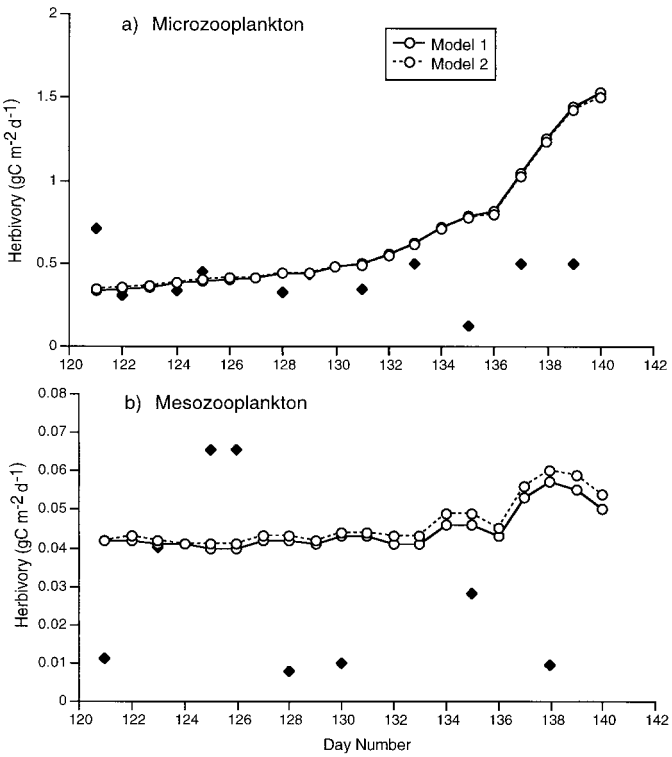

Fig. 5. Modeled zooplankton herbivory compared with observations: (a) daily fluxes of microzooplankton herbivorous grazing (gC m^{-2} d^{-1}) and (b) the same for mesozooplankton.

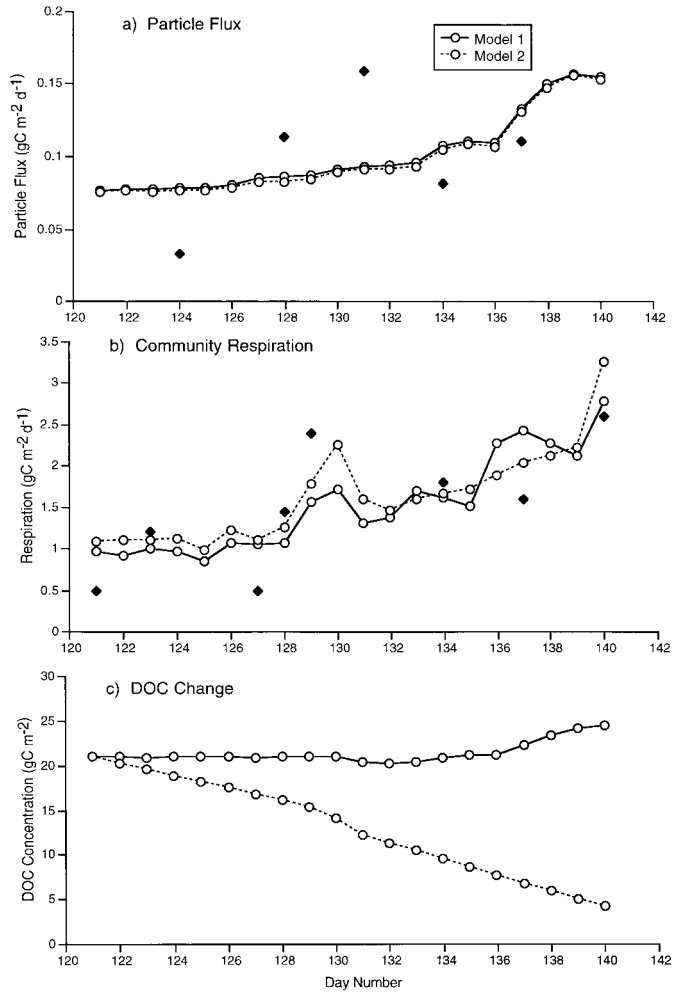

Fig. 6. Modeled (a) downward POC flux (gC m^{-2} d^{-1}) and (b) community respiration (gC m^{-2} d^{-1}) compared with observations. Plot shows the DOC changes predicted by the two models (c).

munity biomass, the modeled community respiration increased over the 20-d period (Fig. 6b) and, apart from days 121 and 127, agreed closely with the observations. The modeled downward POC flux is of the correct magnitude (Fig. 6a), but the paucity and variability of the observations means that we cannot confirm the predicted increase over the period of the experiment. The modeled microphytoplankton sinking rate was 1.5 ± 0.6 m d^{-1} (Table 3); this value may seem low compared with the POC sinking rates of ~100 m d^{-1} estimated from deep sediment traps (Newton et al. 1994), but these rates from the deep traps refer to aggregated senescent material rather then freshly growing phytoplankton.

One of the benefits of this model is that it can be used to analyze the total carbon balance over the whole Lagrangian experiment. If advective fluxes are excluded, the GPP summed over the 20 d should be balanced by the sum of respiration and downward POC flux, plus or minus any net increase or decrease in the concentrations of the phytoplankton, bacteria, zooplankton, and DOC. The result of this accounting exercise for model 1 (Table 4) raises two important points. First, to balance the respiration, the model predicts that the GPP is over twice the measured ^{14}C production of 15.6 gC m^{-2}. This value is achieved by having high values for the fractions of GPP that go to respiration and DOC exudation (Table 3); averaged over the three size classes of phytoplankton, the fraction respired was 0.22 ± 0.15 gC m^{-2} and the fraction going to DOC was 0.34 ± 0.26 gC m^{-2}. Second, modeled DOC increases by 3.5 gC m^{-2} over the 20 d, with most of this increase occurring over the last 5 d (Fig.

Table 4. Overall carbon balance predicted by the two models. For both models the total net primary production was 15.6 gC m^{-2}.

Activity	Total flows (gC m^{-2})* Model 1	Model 2
Input		
Gross primary production	36.6	17.7
Output		
Respiration	27.7	29.3
Downward POC flux	1.8	1.8
Increase in community biomass	3.5	3.3
Increase in DOC	3.5	−16.8
Mesozooplankton mortality (export to higher predators)	0.1	0.1
Total output	36.6	17.7

* For days 121–140.

6c). This increase occurs because the large DOC supply from phytoplankton exudation during the bloom exceeds the demand from bacteria, whose biomass remains virtually constant during the bloom. Because we have no DOC observations, there is no possibility of confirming whether this increase did in fact occur, although other studies have shown that DOC increases during a bloom.

Model 2: DOC unconstrained—The optimized parameter values obtained (Table 3) show some significant differences from the model 1 values. The parameters determining phytoplankton exudation and respiration (c_{i7}, c_{i0}, $i = 1,3$) all have values close to their target values and have SEs that are between 4 and 8 times their estimated values. These high SEs indicate that all these parameters are very poorly determined by the observations, and, in fact, it is possible to obtain as good a fit by setting all these parameters to zero. Thus, the absence of data on DOC has caused the model to be underdetermined in a statistical sense. However, all of the parameters not associated with phytoplankton respiration and exudation were within 2 SEs of the model 1 values (Table 3).

The resulting fit of model 2 to the observations was virtually identical to that of model 1 for most variables (Figs. 3–6), although there were some small differences in the modeled respiration. However, the DOC concentrations were completely different from those of model 1, with DOC declining by 16.8 gC m^{-2} over the 20 d (Fig. 6c). The carbon budget for model 2 is also very different from that of model 1 (Table 4), with GPP only 13% higher that the ^{14}C production. From where then does the carbon come to balance the respiration term? DOC is removed from the DOC pool by the bacteria, and because of the low bacterial GGE (10%), most of this carbon is respired. Thus, in effect the DOC pool is providing a carbon subsidy to the system. However, without any actual DOC observations, we cannot confirm or refute this prediction.

The modeled GGEs for micro- and mesozooplankton and bacteria were 21% ± 10%, 8% ± 9%, and 10% ± 4%, respectively, not significantly different from model 1 values.

Discussion

How well does the model fit the observations?—Before discussing the model results in more detail, the success of the model in reproducing the observations should be assessed. For most of the variables for which we have a good temporal coverage (phytoplankton, bacteria, and community respiration), both models fit the trends over the 20-d period reasonably well (Figs. 3, 4, 6), although the sharp decline in the microphytoplankton bloom in the last few days was not reproduced and the small picoplankton bloom that occurred after day 136 in the model was not apparent in the data. However, bearing in mind the relative simplicity of the model and the fact that the model forcing functions were unsmoothed production estimates obtained from a single daily measurement, it would be unrealistic to expect the model to fit every detail of the temporal changes in phytoplankton. For example, the picoplankton population may have been also grazed by some other unmodeled ecosystem component, such as salps (Fortier et al. 1994).

The assumption of a carbon : chlorophyll ratio of 50 was tested by using a model in which this ratio was a parameter to be optimized rather than a preset value. The results showed that the goodness-of-fit parameter T_{obs} was hardly altered. Furthermore, the estimated value of the carbon : chlorophyll ratio was 47, indicating that our assumed value for this ratio was reasonable, or at least that the model solutions are not very sensitive to the value of this parameter.

The observed bacterial biomass changed very little over time (Fig. 1D), and both models reproduced this finding, apart from days 130–131 when high values of measured bacterial production (Fig. 1D) enabled the modeled bacteria to temporarily escape from microzooplankton grazing control.

The models matched the observed increase in microzooplankton biomass between days 121 and 129, but the lack of good observations for the latter part of the experiment means that the large predicted increase in microzooplankton biomass over this period cannot be confirmed. Similarly, although the general trend of the mesozooplankton observations was matched by the model, the large variability in the observations makes it difficult to draw any firm conclusions about the validity of the model. Both these points emphasize the importance of obtaining high-quality zooplankton data if ecosystem models are to be properly validated.

The model results for mesozooplankton and microzooplankton herbivory (Fig. 5) were within the range of the observations for the majority of the period, but the modeled microzooplankton herbivory was up to 4 times the measured values during the period of the bloom. Microzooplankton herbivory might be expected to increase during a bloom, and so it is puzzling that the observations fail to show any increase. Another check on the validity of the zooplankton model is to calculate the zooplankton ingestion rates and the GGE values for the zooplankton to see whether they are within the range of reasonable values. The modeled range of specific ingestion rates summed over all prey (and GGE) for microzooplankton and mesozooplankton were, respectively, 0.7–1.0 d^{-1} (24%) and 0.3–0.4 d^{-1} (7%) for model 1 and 0.8–1.0 d^{-1} (21%) and 0.3–0.4 d^{-1} (8%) for model 2. The mesozooplankton ingestion rates can be compared with the results of Dam et al. (1993), who measured ingestion rates of mesozooplankton on phytoplankton in the range 0.05–0.6 d^{-1} (approximate average 0.3 d^{-1}) during the JGOFS NABE in 1989. They further estimated that phytoplankton contributed only 50% of the diet of the mesozooplankton, and so their rates must be doubled to get the total ingestion rates; the modeled values are still within the range of observations. The mesozooplankton GGE values are also within the range reported by Parsons et al. (1984). The microzooplankton ingestion rates are well within the range of the NABE results reported by Burkill et al. (1993), but the GGE values are perhaps a little low for protists, which probably make up a large proportion of the microzooplankton (Caron et al. 1985; Verity 1985).

The GGE for bacteria (model 1: 17%, model 2: 10%) is lower than has been assumed in some earlier food web studies (Williams 1981*a*; Fasham 1985), but more recent observations suggest that values between 5% and 20% may in

fact be more typical for bacteria utilizing natural DOC rather than added organic carbon (Kirchman 1990; Connolly et al. 1992; Carlson and Ducklow 1996; Cherrier et al. 1996; Del Giorgio et al. 1997).

The range of values of the modeled flux measurements were all in close agreement with the observed values. This result of the optimization procedure was by no means inescapable. In an earlier version of the model, the microzooplankton were assumed only to graze the pico- and nanophytoplankton, which meant that the microphytoplankton population had to be controlled either by having a high mesozooplankton grazing rate or a high phytoplankton sinking rate leading to a large overestimation of mesozooplankton herbivory or of downward POC flux. Only when the microzooplankton were allowed to feed on all size classes of phytoplankton could the optimized estimates of these two fluxes be brought into broad agreement with the observations. A number of recent studies support the idea of microzooplankton grazing on large phytoplankton (Suttle et al. 1986; Neuer and Cowles 1994).

DOC changes—The two models give very different solutions for the changes in DOC over the 20-d period of the experiment (Fig. 6). In model 2, the DOC pool declined by 16 gC m^{-2}, and this subsidy from the DOC pool together with the GPP balance the measured community respiration (Table 4) via the process of bacterial respiration. In model 1, an attempt was made to avoid this external DOC subsidy by constraining the DOC to be nearly invariant over the whole period. This model produces a DOC increase of 3.2 gC m^{-2} over the 20 d; this increase takes place during the period of the phytoplankton bloom (Fig. 6c), when increased production of DOC by phytoplankton exudation is not balanced by any large increase in bacterial production (Fig. 1D). To achieve this small increase in DOC and balance the community respiration, model 1 assumes much higher values for the fraction of gross production that goes to DOC excretion and respiration (Table 3). The percentage of the gross production of the three size fractions going to DOC was high (33–36%; Table 3) but is well within the range of reported observations (Connolly et al. 1992), especially because this flux includes any effects of viral lysis (Suttle et al. 1990). The high-percentage DOC excretion coupled with phytoplankton respiration at 21–23% of gross production means that the model 1 GPP is 2.3 times the NPP (Table 4). This difference between gross and net production is higher than that often assumed.

The two models gave very different results for the fractions of the DOC input coming from phytoplankton excretion or zooplankton excretion and sloppy feeding. In model 1, the phytoplankton contributed 78% of the DOC supply and the zooplankton contributed 22%, whereas in model 2 the equivalent figures were 17% and 83%. Unfortunately, there does not seem to be a consensus on whether phytoplankton or zooplankton are the major source of DOC. Connolly et al. (1992) considered phytoplankton to be the major source of DOC, a view supported by the modeling study of Anderson and Williams (1998) based on dissolved organic nitrogen and DOC data from the English Channel. However, other workers support the contrary view, that zooplankton are the major source of DOC (Jumars et al. 1989; Banse 1992; Strom et al. 1997). In any event, the importance of these two sources may vary temporally, with phytoplankton excretion being most important during the spring bloom, as the model suggests was the case in 1990, and zooplankton excretion or sloppy feeding being more important in the postbloom period when grazing is more predominant.

Another interesting aspect of model 1 is that it demonstrates that the DOC increases during the bloom occur because the increased supply, mainly from phytoplankton, is not balanced by any increase in the bacterial uptake because the bacteria are kept in check by grazing pressure from microzooplankton. Thingstad et al. (1997) proposed that microzooplankton predation coupled with low bacterial growth can explain the accumulation of DOC during the spring–summer period; our results support this idea.

In the absence of any measurements of DOC during the Lagrangian experiment, we cannot decide definitively between the two possible model solutions. However, results from other studies of DOC seasonal changes favor the first model solution. For example, Williams (1995) analyzed five historical data sets, all of which showed an increase of DOC during the spring–early summer period (*see* Thingstad et al. 1997 for further examples). Using more up-to-date measurement techniques at the Bermuda Atlantic time-series site, Carlson et al. (1994, 1996) showed that by April the DOC had increased by up to 120 mgC m^{-3} from the overwintering concentrations. The change of DOC predicted by model 1 was 99 mgC m^{-3}. Although the Bermuda area is more oligotrophic than the NE Atlantic, the fact that the two estimated DOC increases are similar suggests that the model 1 solution is a more ecologically reasonable representation of the ecosystem carbon fluxes than is model 2.

Zooplankton feeding—If model 1 is accepted as a reasonable description of the carbon flux over the 20 d of the Lagrangian experiment, then this model can be used to investigate ecosystem properties that would have been difficult, if not impossible, to study on the cruise. The first is the composition of the food ingested by the two classes of zooplankton. Figures 7a and 7b partition total micro- and mesozooplankton ingestion into the various sources. The greatest contribution to microzooplankton ingestion is from the nanophytoplankton, with roughly equal contributions from other phytoplankton and bacteria. Averaged over the whole 20 d, the microzooplankton ingestion consisted of 14% picophytoplankton, 51% nanophytoplankton, 20% microphytoplankton, and 15% bacteria.

In the model, mesozooplankton grazed only microphytoplankton and microzooplankton, and averaged over the whole 20 d, microphytoplankton contributed 29% and microzooplankton contributed 71% of the food ingested. The importance of microzooplankton in the diet of larger zooplankters runs counter to the classical idea of mesozooplankters such as copepods being mainly herbivorous. However, recent feeding studies (Dam et al. 1993; Gifford et al. 1995) have shown that many mesozooplankters are in fact omnivorous. For example, the experiments of Dam et al. (1993) that were carried out at the NABE site at 47°N, 17°W in 1989 showed that phytoplankton grazing only accounted for

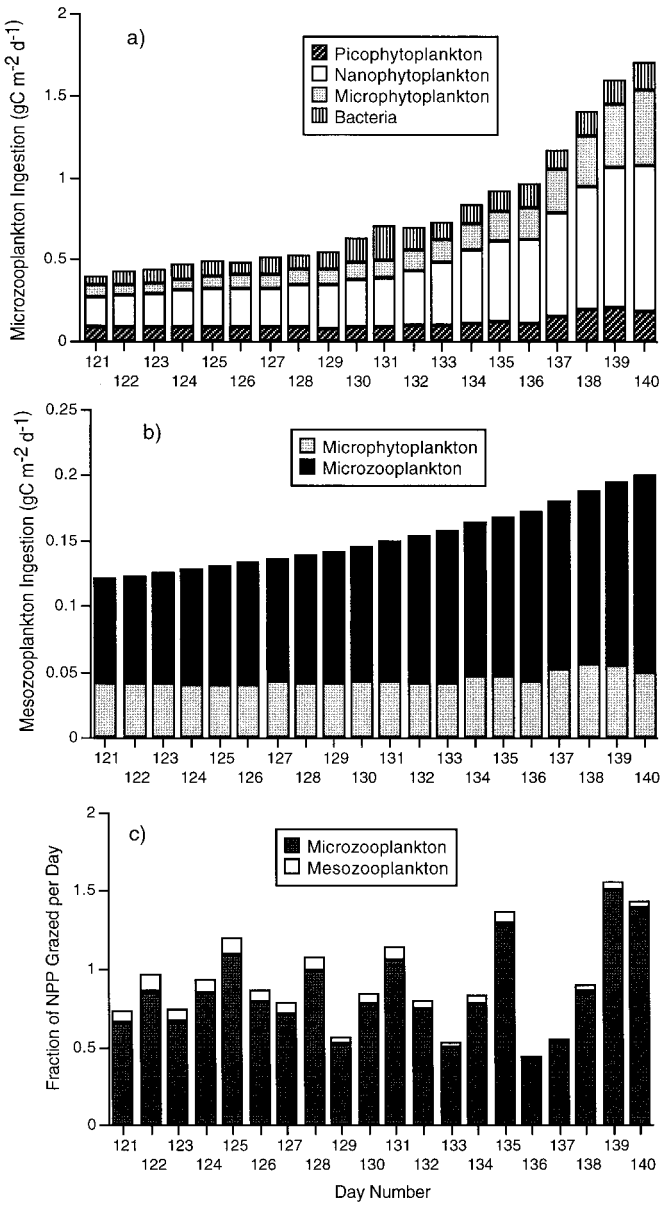

Fig. 7. Composition of food ingested by microzooplankton (a) and mesozooplankton (b). Plot shows the fraction of daily primary production ingested by micro- and mesozooplankton (c). All results for model 1.

around 50% of the respiratory needs of the mesozooplankton, implying that the other 50% is met by feeding on microzooplankton.

Another topical issue is the relative importance of large and small zooplankton in the grazing of phytoplankton. Figure 7c shows the fraction of the daily primary production grazed by these classes of zooplankton. The total fraction grazed changes on a daily basis from 100% to <50%; the lower values occurred mainly during the phytoplankton bloom when the zooplankton grazing rates were unable to keep up with phytoplankton growth rates. Microzooplankters are the dominant herbivores, with an average ratio of mesozooplankton to microzooplankton herbivory of 0.08; such a low proportion has been found in a number of recent process studies in the North Atlantic (Morales et al. 1991; Burkill et al. 1993; Gifford et al. 1995).

The overall carbon budget—The results from the two models give two different scenarios for obtaining a balanced carbon budget. If model 2 is correct, phytoplankton respiration and DOC excretion are small fractions of the GPP, and a large subsidy from the DOC pool over the 20 d is required. However, if the more reasonable model 1 scenario is correct (i.e., there is a small increase in the DOC), phytoplankton respiration and excretion must be large fractions of GPP, resulting in a GPP that is 2.3 times the observed primary production estimate obtained from the 24-h ^{14}C incubations. Obviously, this high ratio of GPP to ^{14}C production could be reduced if it were assumed that the measured community respiration was greatly overestimating the true value, but we have no reason to suspect this to be the case. The comparison made by Bender et al. (1992) of ^{14}C production estimates with gross production obtained from $H_2{}^{18}O$ incubations during the spring bloom at the NABE site at 47°N, 20°W is very useful. They found that the 14-hr ^{18}O estimate of gross production was 1.55-fold greater than the 14-hr ^{14}C estimate and that the latter quantity was 1.25-fold greater than the 24-hr ^{14}C production. Thus, the gross production was 1.94-fold greater than the 24-hr ^{14}C production, which is not very different from the factor of 2.3 obtained from model 1. This fact, coupled with our belief that the model 1 DOC temporal change is more consistent with other observations, leads us to prefer the model 1 carbon budget to that of model 2.

The flow diagram of the model 1 carbon fluxes averaged over the 20-d period are shown in Fig. 8. The first point of interest is the contribution of the various biological components to community respiration (Fig. 9b). Overall, phytoplankton contributed 30% of the respiration, bacteria contributed 38%, and micro- and mesozooplankton is contributed 27% and 5%, respectively. Fifty-seven percent of the respiration came from the organisms <5 μm in size (picophytoplankton, nanophytoplankton, and bacteria), a result that is supported by the size-fractionated respiration measurements made by Williams (1981*b*), who concluded that >50% of the respiration came from organisms in this size class. Heterotrophic organisms contributed 70% of the total respiration, a value somewhat higher than the 60% estimated by Bender et al. (1992) for the 1989 spring bloom at 47°N, 20°W. The DOC uptake by bacteria is quite a high proportion (35%) of the GPP, although because of the low bacterial GGE (17%) the bacterial production was only 6% of GPP (14% of NPP). Furthermore, of the DOC taken up by bacteria 95% is eventually respired, either by bacteria (83%), microzooplankton (10%), or mesozooplankton (2%). These results are comparable to those of the mesocosm experiments of Ducklow et al. (1986), who showed that over a 13-d period, 78% of an added radioactive tracer was respired as CO_2. Our results provide further support for the hypothesis put forward by Ducklow et al. (1986) that heterotrophic bacteria act more as a sink than a link in the marine euphotic zone food web.

The largest contribution to the downward POC flux is

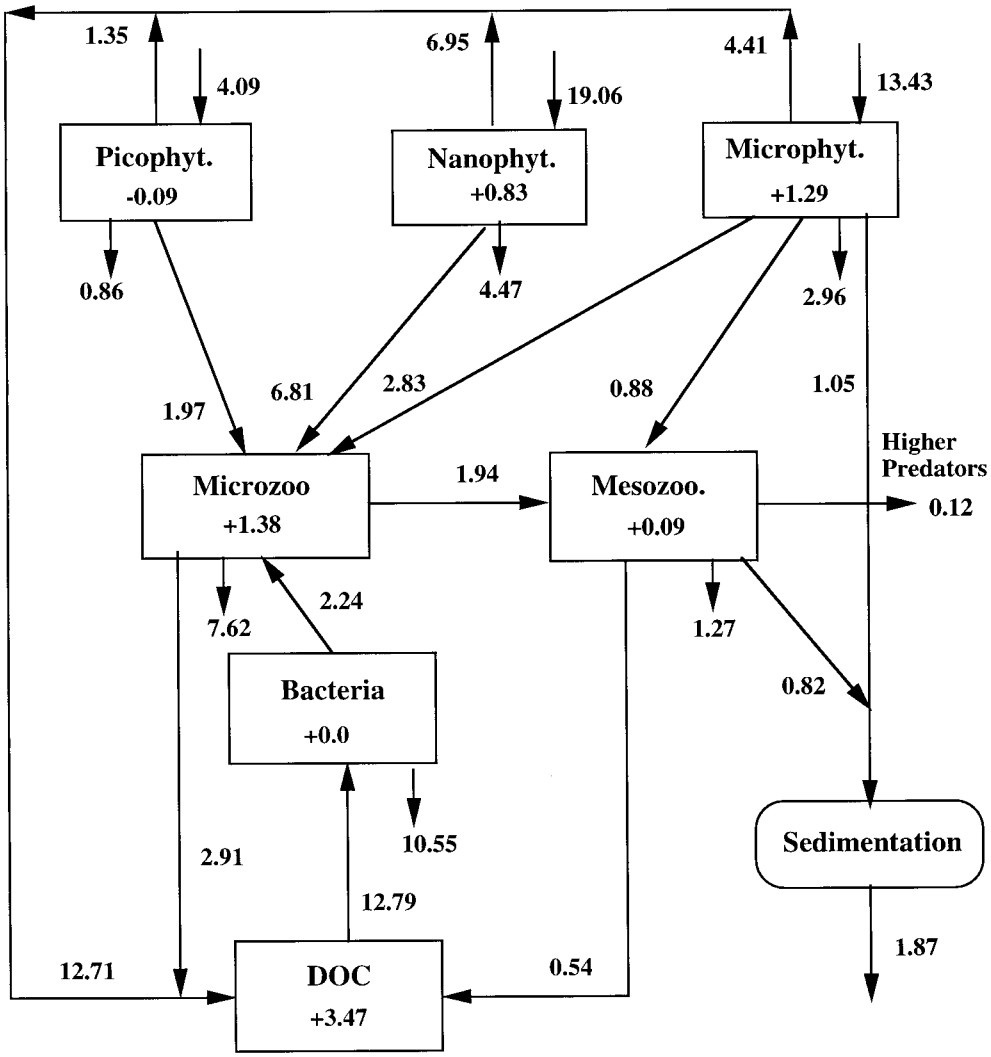

Fig. 8. Daily carbon flows (gC m^{-2} d^{-1}) averaged over the 20-d experiment predicted using model 1. Values within the boxes give the change in standing stock over the same period.

sinking microphytoplankton (56% overall), with mesozooplankton fecal pellets contributing 44% (Fig. 9a). The importance of the sinking of large phytoplankton in the downward POC flux is consistent with the observations that relatively intact diatoms make up a large proportion of recently sedimented material on the ocean floor in the NE Atlantic (Billett et al. 1983). The estimated downward POC flux was only 5% of the GPP, less than half the value estimated by Bender et al. (1992) for the NABE experiment carried out during the spring bloom in the same area the previous year. Sediment trap data from this area of the NE Atlantic analyzed by Newton et al. (1994) showed that the annual average POC flux in 1989 at 3,100 m was 3–4 times higher than that in 1990. Furthermore, Boyd and Newton (1995) showed that the primary production for the 2 yr was broadly comparable, and they attributed the interannual change to differences in the size structure of the dominant phytoplankton species. They used a food web model to show that the relative increase in smaller phytoplankton in 1990 resulted in a POC flux from the surface layer during spring 1990 that was half that for the same period in 1989. The model results presented here support this conclusion.

General conclusions—One of the aims of modern biological oceanography is to quantify the role played by the biotic components of the ecosystem in the flux of carbon and nutrients in the ocean. This objective is hampered both by the complexity of the marine food web and the difficulty of obtaining the necessary observation sets. In this study, we tried to construct a carbon budget for a 20-d period of the spring bloom from the available observations by fitting the data with a size-structured ecosystem model. In a sense, the model was used to combine our prior understanding of the food web with the necessarily imperfect observation set to determine a self-consistent carbon budget. However, it was not possible to obtain a unique solution because of the absence of data on DOC concentrations and, to a lesser extent, inadequate data on micro- and mesozooplankton biomass. This problem highlights the need to improve methods of sampling

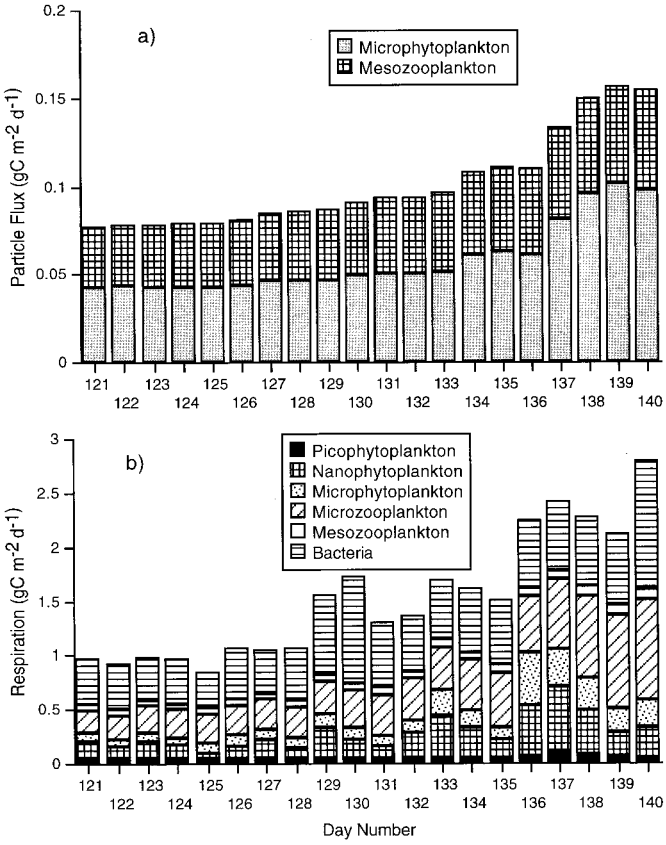

Fig. 9. Sources of downward POC flux (a) and community respiration (b) predicted using model 1.

these variables to achieve a better understanding the carbon budgets of the upper ocean.

Despite these problems, the solution obtained by making the prior assumption that the DOC concentration should remain broadly constant over the period of the cruise (model 1) predicted a DOC change during the period of the phytoplankton bloom that is consistent with observations from other areas. However, to achieve a balanced budget for this case it was necessary to assume that gross primary production was over twice that determined by the ^{14}C measurements and that a high proportion of this gross production was exuded as DOC by the phytoplankton. The uptake and respiration of this DOC by bacteria with a low growth efficiency then makes a major contribution to the community respiration. The bacteria are acting more as a sink in the food web than a link to higher trophic levels, and there is supporting evidence for this view of how carbon flows through the euphotic zone. The results of this study strongly indicate the need for further observational programs in which the sampling strategy is specifically targeted to resolving these issues.

Another important result of this work was that the different roles in the ecosystem played by small and large organisms could be quantified; the small phytoplankton (<5 μm), bacteria, and microzooplankton made the major contribution to the community respiration, and the large phytoplankton and mesozooplankton were the source of the downward POC flux. These findings show the importance of size structure for the future development of generic ecosystem models.

References

ANDERSON, T. R., AND P. J. L. WILLIAMS. 1998. Modelling the seasonal cycle of dissolved organic carbon at station El in the English Channel, Est. Coastal Shelf Sci. **46:** 93–109.

BANSE, K. 1992. Grazing, temporal changes of phytoplankton concentrations, and the microbial loop in the open sea, p. 409–440. *In* P. G. Falkowski and A. D. Woodhead [eds.], Primary productivity and biogeochemical cycles in the sea. Plenum.

BENDER, M. L., H. W. DUCKLOW, J. KIDDON, J. MARRA, AND J. H. MARTIN. 1992. The carbon balance during the 1989 spring bloom in the North Atlantic Ocean at 47°N 20°W. Deep-Sea Res. **39:** 1707–1725.

BERGGEREN, E., B. HANSEN, AND T. KIØRBOE. 1988. Food size spectra, ingestion and growth of the copepod *Acartia tonsa* during development: Implications for determination of copepod production. Mar. Biol. **99:** 341–352.

BILLETT, D. S. M., R. S. LAMPITT, A. L. RICE, AND R. F. C. MANTOURA. 1983. Seasonal sedimentation of phytoplankton to the deep-sea benthos. Nature **302:** 520–522.

BOYD, P. W., S. J. BURY, N. J. P. OWENS, G. J. SAVIDGE, AND T. PRESTON. 1995. A comparison of isotopic and chemiluminescent methods of estimating microalgal nitrate uptake in the NE Atlantic. Mar. Ecol. Prog. Ser. **116:** 199–205.

———, AND P. NEWTON. 1995. Evidence of the potential influence of planktonic community structure on the interannual variability of particulate organic carbon flux. Deep-Sea Res. **42:** 619–639.

BURKILL, P. H., E. S. EDWARDS, A. W. G. JOHN, AND M. A. SLEIGH. 1993. Microzooplankton and their herbivorous activity in the northeastern Atlantic Ocean. Deep-Sea Res. **40:** 479–494.

CARLSON, C. A., AND H. W. DUCKLOW. 1996. Growth of bacterioplankton and consumption of dissolved organic carbon in the Sargasso Sea. Aquat. Microb. Ecol. **10:** 69–85.

———, ———, AND A. F. MICHAELS. 1994. Annual flux of dissolved organic carbon from the euphotic zone in the northwestern Sargasso Sea. Nature **371:** 405–408.

———, ———, AND T. D. SLEETER. 1996. Stocks and dynamics of bacterioplankton in the northwestern Sargasso Sea. Deep-Sea Res. **43:** 491–515.

CARON, D. A., J. C. GOLDMAN, O. K. ANDERSEN, AND M. R. DENNETT. 1985. Nutrient cycling in a microflagellate food chain. II. Population dynamics and carbon cycling. Mar. Ecol. Prog. Ser. **24:** 243–254.

CHERRIER, J., J. E. BAUER, AND E. R. M. DRUFFEL. 1996. Utilization and turnover of labile dissolved organic matter by bacterial heterotrophs in eastern North Pacific surface waters. Mar. Ecol. Prog. Ser. **139:** 267–279.

CHIPMAN, D. W., J. MARRA, AND T. TAKAHASHI. 1993. Primary production at 47°N 20°W in the North Atlantic ocean: A comparison between the ^{14}C incubation method and the mixed layer carbon budget. Deep-Sea Res. **40:** 151–170.

CONNOLLY, J. P., R. B. COFFIN, AND R. E. LANDBECK. 1992. Modeling carbon utilization by bacteria in natural water systems, p. 249–276. *In* C. J. Hurst [ed.], Modelling the metabolic and physiologic activities of micro-organisms. Wiley.

DAM, H. G., C. A. MILLER, AND S. H. JONASDOTTIR. 1993. The trophic role of mesozooplankton at 47°N during the North Atlantic Bloom Experiment. Deep-Sea Res. **40:** 197–212.

DEL GIORGIO, P. A., J. J. COLE, AND A. CIMBLERIS. 1997. Respiration rates in bacteria exceed phytoplankton production in unproductive aquatic systems. Nature **385:** 148–151.

DUCKLOW, H. W., AND M. J. R. FASHAM. 1991. Bacteria in the greenhouse: Modeling the role of oceanic plankton in the global carbon cycle, p. 1–31. *In* R. Mitchell [ed.], New concepts in environmental microbiology. Wiley-Liss.

———, ———, AND A. VEZINA. 1989. Flow analysis of open sea plankton networks, p. 159–205. *In* F. Wulff, J. G. Field, and K. H. Mann [eds.], Network analysis in marine ecology. Springer-Verlag.

———, D. A. PURDIE, P. J. L. WILLIAMS, AND J. M. DAVIES. 1986. Bacterioplankton: A sink for carbon in a coastal marine plankton community. Science **232:** 865–867.

FASHAM, M. J. R., 1985. Flow analysis of materials in the marine euphotic zone. Can. Bull. Fish. Aquat. Sci. **213:** 139–162.

———, AND G. T. EVANS. 1995. The use of optimisation techniques to model marine ecosystem dynamics at the JGOFS station at 47°N 20°W. Philos. Trans. R. Soc. Lond. **B348:** 206–209.

———, AND ———. 1998. Advances in ecosystem modelling within JGOFS. *In* H. W. Ducklow, J. G. Field, and R. Hanson [eds.], The changing ocean carbon cycle: A mid-term synthesis of the Joint Global Ocean Flux Study. Cambridge University Press, (in press).

FORTIER, L., J. LE FÈVRE, AND L. LEGENDRE. 1994. Export of biogenic carbon to fish and to the deep ocean: The role of large planktonic microphages. Limnol. Oceanogr. **16:** 809–839.

GIESKES, W. W. C. 1991. Algal pigment fingerprints: Clues to taxon-specific abundance, productivity and degradation of phytoplankton in seas and oceans, p. 61–101. *In* S. Demers [ed.], Particle analysis in oceanography. Springer-Verlag.

GIFFORD, D. J., E. MARTIN, L. M. FESSENDEN, AND P. R. GARRAHAN. 1995. Grazing by microzooplankton and mesozooplankton in the high-latitude North Atlantic Ocean: Spring versus summer dynamics. J. Geophys. Res. **100:** 6665–6675.

GILL, P. E., W. MURRAY, AND M. H. WRIGHT. 1981. Practical optimization. Academic Press.

HOLLIGAN, P. M., R. D. PINGREE, AND G. T. MARDELL. 1985. Oceanic solitons, nutrient pulses and phytoplankton growth. Nature **314:** 348–350.

JOINT, I. R., AND R. WILLIAMS. 1985. Demands of the herbivore community on phytoplankton production in the Celtic Sea in August. Mar. Biol. **87:** 297–306.

JUMARS, P. A., D. L. PENRY, J. A. BAROSS, M. J. PERRY, AND B. W. FROST. 1989. Closing the microbial loop: Dissolved carbon pathway to heterotrophic bacteria from incomplete ingestion, digestion and absorption in animals. Deep-Sea Res. **36:** 483–495.

KIRCHMAN, D. L. 1990. Limitation of bacterial growth by dissolved organic matter in the subarctic Pacific. Mar. Ecol. Prog. Ser. **62:** 47–54.

———, R. G. KEIL, M. SIMON, AND N. A. WELSCHMEYER. 1993. Biomass and production of heterotrophic bacterioplankton in the oceanic subarctic Pacific. Deep-Sea Res. **40:** 967–988.

LAWS, E. A. 1991. Photosynthetic quotients, new production and net community production in the open ocean. Deep-Sea Res. **38:** 143–167.

MORALES, C. E., A. BEDO, R. P. HARRIS, AND P. R. G. TRANTER. 1991. Grazing of copepod assemblages in the north-east Atlantic: The importance of the small size fraction. J. Plankton Res. **13:** 455–472.

———, R. P. HARRIS, R. N. HEAD, AND P. R. G. TRANTER. 1993. Copepod grazing in the oceanic northeast Atlantic during a 6 week drifting station: The contribution of size classes and vertical migrants. J. Plankton Res. **15:** 185–211.

NEUER, S., AND T. J. COWLES. 1994. Protist herbivory in the Oregon upwelling system. Mar. Ecol. Prog. Ser. **113:** 147–162.

NEWTON, P. P., R. S. LAMPITT, T. D. JICKELLS, P. KING, AND C. BOUTLE. 1994. Temporal and spatial variability of biogenic particle fluxes during the JGOFS northeast Atlantic. Deep-Sea Res. **41:** 1617–1642.

PARSONS, T., M. TAKAHASHI, AND B. HARGRAVE. 1984. Biological oceanographic processes, 3rd ed. Pergamon.

PRESS, W. H., S. A. TEUKOLSKY, W. T. VETTERLING, AND B. P. FLANNERY. 1992. Numerical recipes in C. Cambridge University Press.

RITCHIE, G. D., AND G. B. SHIMMIELD. 1991. The use of $^{210}Po/^{210}Pb$ disequilibria in the determination of the fate of marine particulate matter, p. 142–153. *In* P. J. Kershaw and D. S. Woodhead [eds.], Radionuclides in the study of marine processes. Elsevier.

SAVIDGE, G., P. BOYD, A. POMROY, D. HARBOUR, AND I. JOINT. 1995. Phytoplankton production and biomass estimates in the northeast Atlantic Ocean, May–June 1990. Deep-Sea Res. **42:** 599–617.

———, AND OTHERS. 1992. The BOFS 1990 spring bloom experiment: Temporal evolution and spatial variability of the hydrographic field. Prog. Oceanogr. **29:** 235–281.

SIEBURTH, J. M., V. SMETACEK, AND J. LENZ. 1978. Pelagic ecosystem structure: Heterotrophic compartments of the plankton and their relationship to plankton size fractions. Limnol. Oceanogr. **23:** 1256–1263.

STOECKER, D. K. 1984. Particle production by planktonic ciliates. Limnol. Oceanogr. **29:** 930–940.

STROM, S., R. BENNER, S. ZIEGLER, AND M. DAGG. 1997. Planktonic grazers are a potentially important source of marine dissolved organic carbon. Limnol. Oceanogr. **42:** 1364–1374.

SUTTLE, C. A., A. M. CHAN, AND M. T. COTTRELL. 1990. Infection of phytoplankton by viruses and reduction of primary productivity. Nature **347:** 467–469.

———, ———, W. D. TAYLOR, AND P. J. HARRISON. 1986. Grazing of planktonic diatoms by microflagellates. J. Plankton Res. **8:** 393–398.

TAYLOR, A. H., D. S. HARBOUR, R. P. HARRIS, P. H. BURKILL, AND E. S. EDWARDS. 1993. Seasonal succession in the pelagic ecosystem of the North Atlantic and the utilization of nitrogen. J. Plankton Res. **15:** 875–891.

THINGSTAD, T. F., Å. HAGSTRÖM, AND F. RASSOULZADEGAN. 1997. Accumulation of degradable DOC in surface waters: Is it caused by a malfunctioning microbial loop? Limnol. Oceanogr. **42:** 398–404.

VERITY, P. G. 1985. Grazing, respiration, and growth rates of tintinnids. Limnol. Oceanogr. **30:** 1268–1282.

WILLIAMS, P. J. L. 1981*a*. Incorporation of microheterotrophic processes into the classical paradigm of the planktonic food web. Kiel. Meeresforsch. **5:** 1–28.

———. 1981*b*. Microbial contribution to overall marine metabolism: Direct measurements of respiration. Oceanol. Acta **4:** 359–364.

———. 1995. Evidence for the seasonal accumulation of carbon-rich dissolved organic material, its scale in comparison with changes in particulate material and the consequential effect on net C/N assimilation ratios. Mar. Chem. **51:** 17–29.

Received: 9 February 1998
Accepted: 22 July 1998
Amended: 14 September 1998